

THE ANALYTICAL MODEL OF THE HELICAL ACCELERATING STRUCTURE OF LINAC WITH HELIX OUTSIDE OF THE VACUUM CHAMBER

N.V. Avrelina[†], TRIUMF, Vancouver, Canada

Abstract

An analytical model of the helical RF resonator for the single charged 250 keV nitrogen ion implanter operating in CW was developed. The analytical model allowed to determine the geometry of the accelerating structure and to construct CST Microwave Studio and ANSYS HFSS models based on this analytical model. Results obtained from the analytical model and simulations were within 5% of each other. The experimental investigation of the accelerating section confirmed that the models are correct. The accelerating section was tuned and verified for the right accelerating field distribution and operating frequency. Finally, the section was successfully tested in 2 kW CW RF power.

INTRODUCTION

The analytical model of the helical accelerating structure with the helix outside of the vacuum chamber was developed for the single charged 250 keV nitrogen ion implanter where the relative injection speed of ions is $\beta_{inj} = 0.0021$ and relative final speed of ions is $\beta_{exit} = 0.0062$ [1]. The photo in the Fig. 1 shows the helical accelerating structure with open upper compartment, where the helix is located.



Figure 1: The 250 keV Implanter of single charged nitrogen ions.

THE DESIGN OF THE RF RESONATOR

Given a rather low operating frequency of 13.56 MHz and given the goal of reducing the size of an accelerating structure, the resonator of a helical type loaded by an accelerating channel was selected in the design. The accelerating channel is composed of 10 drift tubes and is operating in π mode. These tubes are connected to the two longitudinal bars, which are then connected to the ends of the half-wave length helical elements of the resonator. The photo of the open resonator is presented in Fig. 2.

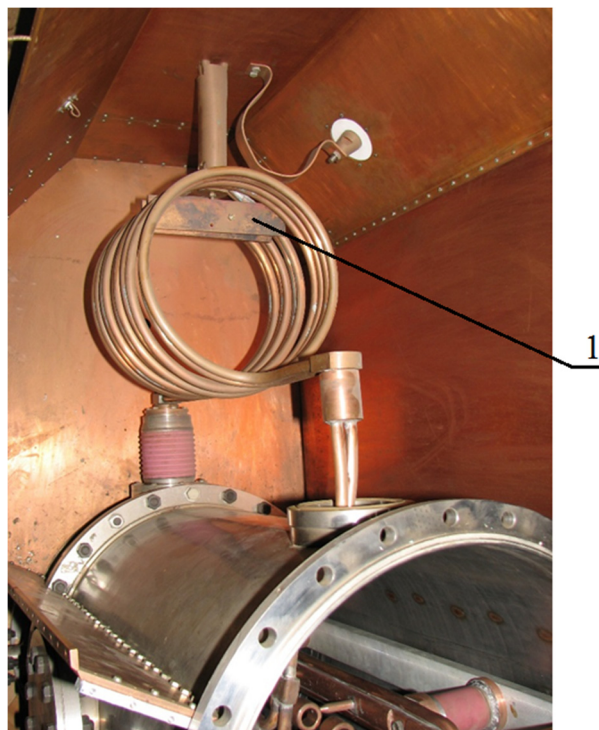


Figure 2: The opened resonator with the helical part that is connected to the accelerating channel via a vacuum feedthrough (the front feedthrough has removed to show the shape of conductor).

To tune the resonance frequency of this resonator, two plates were used to shorten the windings (pos. 1).

The helical element was constructed out of two 12 mm diameter copper pipes that were soldered together. These pipes are water cooled. They are connected through the feedthrough insulators (Fig. 3) with the two bars that support the drift tubes. S.A. Vekshinski Research Institute of Vacuum Technologies in Moscow has manufactured these vacuum feedthroughs from alumina. The helical element could be easily disconnected and replaced by another one, as these connections (Fig. 3) are located outside of the vacuum chamber. Moreover, those connectors are of the flange type, which provide good RF connection and prevent water leaks. The indium gaskets (pos. 7) make good electrical connections and the rubber gaskets (pos. 8) are used for water seal connections. Compressed by a flange (pos. 1), the vacuum rubber gasket (pos. 2) provides vacuum sealing.

Content from this work may be used under the terms of the CC BY 3.0 licence (© 2018). Any distribution of this work must maintain attribution to the author(s), title of the work, publisher, and DOI.

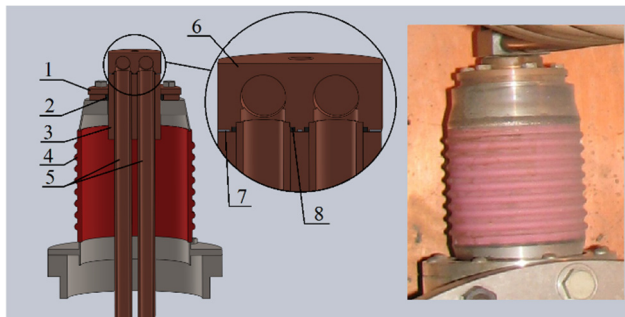


Figure 3: The design of the vacuum feedthrough.

The accelerating channel consists of 10 drift tubes with outer and inner diameters of 30 mm and 18 mm. The accelerating channel was designed to be inside a cradle (Fig. 4) which allows assembly of this channel outside of the vacuum chamber.

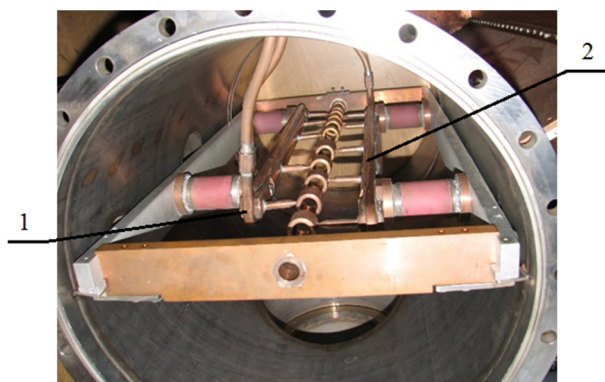


Figure 4: The accelerating channel of the implanter.

ANALYTICAL MODEL OF THE ACCELERATING STRUCTURE

The design and optimization of the accelerating structure were done in the following steps: the analytical model, the study of the scalable mock-up of the resonator [1], simulations of the structure in the CST Microwave Studio and ANSYS Workbench followed by the experimental measurements and tests.

The analytical model helped to estimate the dimensions of the accelerating structure and to optimize its electrodynamic characteristics. The structure was represented as a resonator that consists of piece of a transmission line with a helical element instead of the inner conductor, shorted on the one end and connected to a capacitor and an inductor in series on the other end. The capacitor and the inductor represent the capacitance of the accelerating channel and the inductance of the two leads of the helical element. In the first approach this transmission line was running in the TEM mode. For the simulation, this half wavelength resonator was represented as two quarter wavelength resonators. The equivalent circuit of the quarter wavelength resonator is represented in Fig. 5. There C_{vf} represents the capacitance of the vacuum feedthrough, L_{lead1} and L_{lead2} are the inductances of a lead of the helical element, before and after the vacuum feedthrough, respectively.

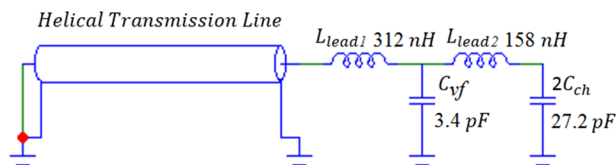


Figure 5: The model of the transmission line and the equivalent circuit of the resonator.

The helical element allows to significantly reduce the dimensions of the accelerating structure. To simulate a resonator that is based on a transmission line with a helical inner conductor, we have calculated its characteristic impedance Z_0 , propagation constant γ and losses α_{loss} . In the model, an unwrapped ribbon helix was used for an equivalent representation of the transmission line geometry [2, 3] (Fig. 6).

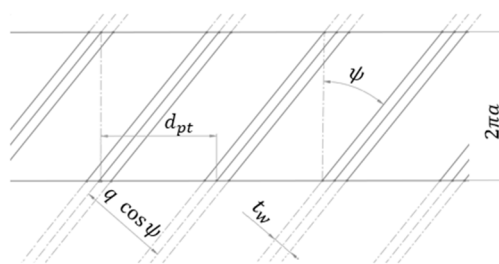


Figure 6: The model of the helical transmission line.

The model allows to find the characteristic impedance Z_0 and to minimize the losses in the transmission line for different pitches and cross-sections of its helical conductor. The formula to determine α_{loss} is given by:

$$\alpha_{loss} = \frac{4}{\pi \sin \theta} \frac{F\left(\frac{\pi}{2}, \cos \theta\right)}{P_{-q}(\cos \theta) P_{-q}(\cos \theta')} \frac{R_0}{2Z_0}, \quad (1)$$

where

$$Z_0 = \frac{1}{4} \sqrt{\frac{\mu_0}{\epsilon_0}} \frac{1}{\sin(q\pi)} \frac{P_{-q}(\cos(\theta'))}{P_{-q}(\cos(\theta))}$$

$F\left(\frac{\pi}{2}, \cos \theta\right)$ is the elliptical Integral of the first kind,

$$P_q(\cos \theta) = \frac{\sin(q\pi)}{\pi} \sum_{m=0}^{\infty} (-1)^m \left(\frac{1}{q-m} - \frac{1}{q+m+1} \right) P_m(\cos \theta)$$

$P_m(\cos \theta)$ are the Legendre polynomials,

$$\theta = \pi - \theta', \quad \theta = \frac{\pi t_w}{d_{pt}}, \quad q = k a \cos(\psi), \quad k = \frac{2\pi f_0}{c},$$

$$f_0 \text{ is the operating frequency, } R_0 = \sqrt{\frac{4\pi f_0 \mu_0}{2\pi a \sigma_{cu} \cos^2(\psi)}},$$

a is the radius of helical element, σ_{cu} is the conductance of copper, ψ is the angle of helical turns.

The plot of α_{loss} is presented in (Fig. 7). The minimal losses correspond to the ratio of conductor width and helical pitch of 0.54. The conductor width was selected based on a compromise between the losses and dimensions of the whole accelerating structure to be $\frac{t_w}{d_{pt}} = 0.795$.

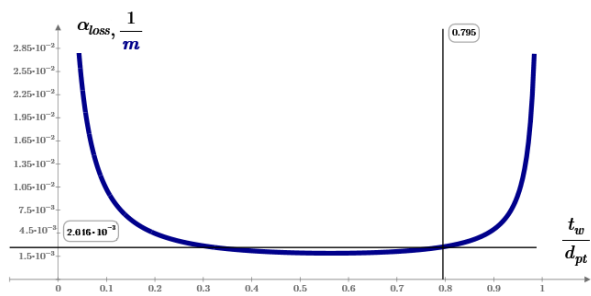


Figure 7: Losses of helical transmission line.

The accelerating channel capacitance was calculated using electrostatic solver in Comsol [4]. As per this calculation, the capacitance between terminals (Fig. 4, pos. 1 and pos. 2) was found to be $C_{ch} = 13.6 \text{ pF}$. As per the equivalent circuit presented in Fig. 5 and the model, the calculated length of the whole helical element was found to be 175 mm and the optimal helical pitch to be 30.2 mm .

SIMULATION OF ACCELERATING STRUCTURE IN ANSYS WORKBENCH

ANSYS Workbench allowed to study of the 3D model of this accelerating structure. Figure 8 shows the electrical field distribution in the vertical plane of the structure (simulated using HFSS eigen mode).

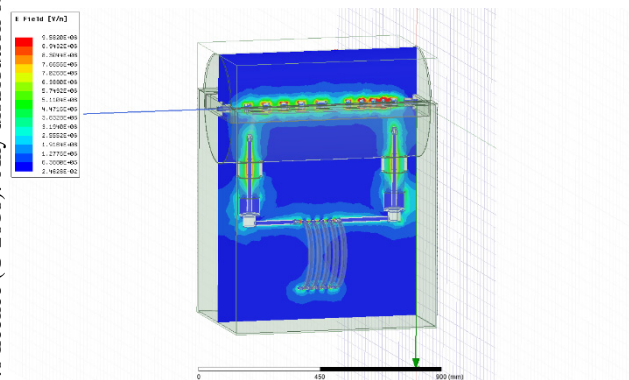


Figure 8: Electrical field in the structure.

The capacitor C_{vf} in the equivalent circuit (Fig. 5) confirms the presence of higher field near the vacuum feed-throughs.

The steady-state thermal solver of ANSYS Workbench gave the temperature distribution in the structure (Fig. 9).

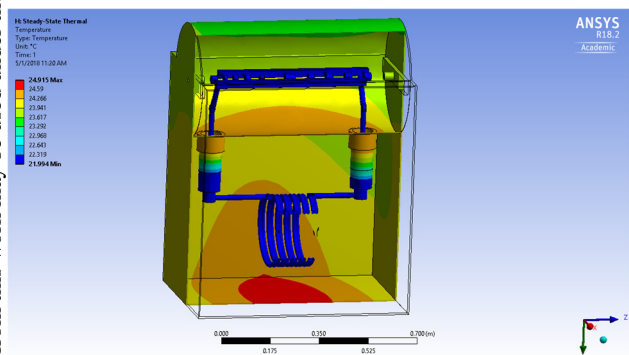


Figure 9: Temperature distribution in the structure.

The water of 22°C was used for cooling the helix, it leads and two bars of the accelerating channel. Ambient air film coefficient at temperature 22°C was $5 \text{ W}/\text{m}^2\text{C}$. The maximum temperature in the structure is below 36°C .

EXPERIMENTAL STUDY OF THE ACCELERATING STRUCTURE

Following the experimental investigation of the mock-up accelerating structure, the full scale accelerating resonator was manufactured and studied. The frequency of this resonator was adjusted to 13.56 MHz using the shortening plates (Fig 2, pos. 1). The Q_l factor was measured using the method of resonator phase shift and the resulting value was $Q_l = 1100$. The experimental investigation and the CST Microwave Studio simulation results of the accelerating field distribution are presented in Fig. 10.

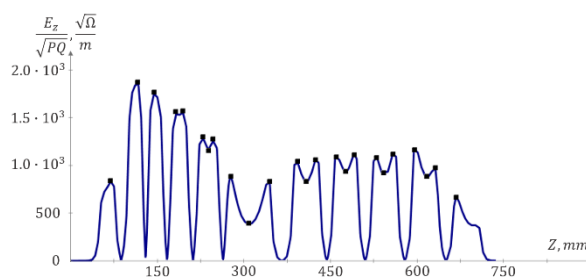


Figure 10: The distribution of E_z in the accelerating channel and the experimental extremal points (marked as “■”) before the hot test.

Post processing calculations determined that $R_{sh} = 167 \frac{\text{M}\Omega}{\text{m}}$ and $R_{eff\ sh} = 132 \frac{\text{M}\Omega}{\text{m}}$. Taking into account measured R_{sh} and beam dynamic calculations, only 1.5 kW of RF power were required to form the accelerating field. The high-power test of the accelerating structure showed that the structure could operate at the level above 2 kW of CW RF power.

CONCLUSION

The experimental study of the accelerating structure of the implanter showed that it has high $R_{sh\ eff}$ and Q_l factor. This accelerating structure could be used in the implanter to accelerate ions of different types and it could be run using a CW RF amplifier with power less than 2 kW .

REFERENCES

- [1] N.V. Avreline, S.M. Polozov, A.G. Ponomarenko, “The study of the helical RF resonator for the 300 keV nitrogen ion CW implanter,” Proceedings of RuPAC2016, St. Petersburg, Russia.
- [2] R.A Silin, V.P. Sazonov, “Moderating Systems,” Sov. Radio, 1966.
- [3] Chiao-Min Chu, “Propagation of wave in helical guides,” Journal of Applied Physics, vol.29, number 1, January, 1958, pp. 88-99.
- [4] COMSOL, <https://www.comsol.com/>

Content from this work may be used under the terms of the CC BY 3.0 licence (© 2018). Any distribution of this work must maintain attribution to the author(s), title of the work, publisher, and DOI.